RESEARCH ARTICLE

WILEY

Season-based rainfall–runoff modelling using the probability-distributed model (PDM) for large basins in southeastern Brazil

Rong Zhang[1] [iD] | Luz Adriana Cuartas[1] | Luiz Valerio de Castro Carvalho[1] |
Karinne Reis Deusdará Leal[1] | Eduardo Mário Mendiondo[1,2] | Narumi Abe[1,2] |
Stephen Birkinshaw[3] | Guilherme Samprogna Mohor[1] | Marcelo Enrique Seluchi[1] |
Carlos Afonso Nobre[1,4]

[1] CEMADEN (National Center for Monitoring and Early Warning of Natural Disasters), Estrada Doutor Altino Bondesan, 500—Distrito de Eugênio de Melo, São José dos Campos, São Paulo, Brazil

[2] São Carlos School of Engineering, EESC-USP, University of São Paulo, São Carlos, São Paulo, Brazil

[3] Water Resource Systems Research Laboratory, School of Civil Engineering and Geosciences, Newcastle University, Newcastle upon Tyne NE1 7RU, UK

[4] Earth System Science Center, National Institute for Space Research (CCST/INPE), São José dos Campos, São Paulo, Brazil

Correspondence
Rong Zhang, CEMADEN (Centro Nacional de Monitoramento e Alertas de Desastres Naturais), Estrada Doutor Altino Bondesan, 500—Distrito de Eugênio de Melo, São José dos Campos, São Paulo, Brazil.
Email: rong.zhang@cemaden.gov.br; zhangrong.research@outlook.pt

Funding information
National Council for Scientific and Technological Development, Grant/Award Numbers: #465501/2014-1, DTI-A-371291/2016-0, DTI-A-382737/2015-6, DTI-A-550022/2014-7, DTI-B-382165/2015-2, PCI-DB-300463/2016-2, PCI-DB-312503/2016-4 and PCI-DC-300702/2016-7; São Paulo Research Foundation, Grant/Award Number: #2014/50848-9

Abstract

Southeastern Brazil is characterized by seasonal rainfall variability. This can have a great social, economic, and environmental impact due to both excessive and deficient water availability. During 2014 and 2015, the region experienced one of the most severe droughts since 1960. The resulting water crisis has seriously affected water supply to the metropolitan region of São Paulo and hydroelectric power generation throughout the entire country. This research considered the upstream basins of the southeastern Brazilian reservoirs Cantareira (2,279 km^2; water supply) and Emborcação (29,076 km^2), Três Marias (51,576 km^2), Furnas (52,197 km^2), and Mascarenhas (71,649 km^2; hydropower) for hydrological modelling. It made the first attempt at configuring a season-based probability-distributed model (PDM-CEMADEN) for simulating different hydrological processes during wet and dry seasons. The model successfully reproduced the intra-annual and interannual variability of the upstream inflows during 1985–2015. The performance of the model was very satisfactory not only during the wet, dry, and transitional seasons separately but also during the whole period. The best performance was obtained for the upstream basin of Furnas, as it had the highest quality daily precipitation and potential evapotranspiration data. The Nash–Sutcliffe efficiency and logarithmic Nash–Sutcliffe efficiency were 0.92 and 0.93 for the calibration period 1984–2001, 0.87 and 0.88 for the validation period 2001–2010, and 0.93 and 0.90 for the validation period 2010–2015, respectively. Results indicated that during the wet season, the upstream basins have a larger capacity and variation of soil water storage, a larger soil water conductivity, and quicker surface water flow than during the dry season. The added complexity of configuring a season-based PDM-CEMADEN relative to the traditional model is well justified by its capacity to better reproduce initial conditions for hydrological forecasting and prediction. The PDM-CEMADEN is a simple, efficient, and easy-to-use model, and it will facilitate early decision making and implement adaptation measures relating to disaster prevention for reservoirs with large-sized upstream basins.

KEYWORDS

2014/2015 water crisis, intra-annual and interannual rainfall variability, PDM-CEMADEN, seasonal calibration, southeastern Brazil

1 | INTRODUCTION

Large intra-annual rainfall variability is one of the main climate characteristics in southeastern Brazil (Figure 1 in Grimm, 2011), where around 80% of annual rainfall occurs during the period from November to March; and, as a consequence, around 68% of annual river discharges are produced during the period from December to April. Interannual rainfall variability is also considerable; annual rainfall may oscillate between 0.6 and 1.4 times the climatological mean; as a result, annual river discharges may range between 0.3 and 2.0 times the mean. The large intra-annual and interannual variability has posed great challenges for an appropriate water resources management strategy (Fan, Collischonn, Meller, & Botelho, 2014; Nobre, Marengo, Seluchi, Cuartas, & Alves, 2016). Furthermore, rainfall and river discharges within the region have decreased significantly over the last 30 years, which has had a great impact on hydroelectric generation and agricultural production (Rao, Franchito, Santo, & Gan, 2016). According to Rao et al. (2016), rainfall of the region has decreased around 5 mm/year (or 165 mm in total) for both the annual and wet seasons in the period 1979–2011; and inflows to most hydroelectric dams of the region have decreased around 20% for the same period. Since the austral summer of 2014, the region has suffered from one of the most severe droughts in the most recent five decades (Coelho, Cardoso, & Firpo, 2016; Getirana, 2016; Nobre et al., 2016). The Cantareira reservoir system reached its lowest historical storage levels in January 2015 with only 5% of its 1.3 billion m^3 capacity and 15% at the end of the rainy season in March 2015 (Nobre et al., 2016).

The probability-distributed model (PDM; Moore, 2007; Moore & Bell, 2002) has been widely tested all over the world for its capacity for short-term flood forecasting (up to 10 days; Liu et al., 2015; Moore, 1999) and long-term runoff prediction (up to 1 year; Cabus, 2008; McIntyre, Lee, Wheater, Young, & Wagener, 2005) at a catchment scale. By coupling it with an atmospheric model, Best et al. (2011) developed the Joint UK Land Environment Simulator, for a continental scale, for both operational weather forecasting and climate change simulations. The potential application of the model to Brazilian catchments for natural disaster purposes is very interesting due to its characteristic of being simple, efficient, and easy to use, with a low demand on input data, parameters, and computational resources. It makes possible effective and efficient runoff forecasting and prediction, which means that potential economic, social, and environmental losses can be avoided or substantially reduced by appropriately made and timely implemented adaptation measures. However, considering the lumped nature of the model, there are tremendous challenges to its reliability in reproducing the large intra-annual and interannual hydrological variability for large basins.

Traditional hydrological simulations consider a unique parameter set for the entire simulation period. Hydrological variation is then captured by the input variables such as precipitation and potential evapotranspiration (PET) and model formulation. However, hydrological model parameters can be time varying, which may be a result of catchment change (such as land use/vegetation change), climate variability, and climate change (such as change of precipitation/

evapotranspiration dynamics of vegetation due to higher or lower temperatures; Kim & Han, 2017). So hydrological variation can be captured in models by time-varying model parameters and nonstationary hydrological model structure and catchment characteristic changes such as land use and vegetation variations (Merz, Parajka, & Blöschl, 2011). Paik, Kim, Kim, and Lee (2005), de Vos, Rientjes, and Gupta (2010), Luo, Wang, Shen, Zheng, and Zhang (2012), Seiller, Anctil, and Perrin (2012), Kim and Lee (2014), Zhang, Chen, Yao, and Lin (2015), and Kim, Kwon, and Han (2016) demonstrated that subannual calibration can improve simulations of the temporal variations of the varying catchment conditions within the year over a traditional calibration scheme, because the time-varying model parameters can consider nonstationary climate and land use conditions. Kim and Han (2017) recommended the use of an optimal calibration period with a trade-off between model performance and parameter settings variance for subannual calibration; as well, they suggested the selection of a calibration method (e.g., in series or in parallel) based on the purpose of model usage.

This study intends to test the hypothesis that different hydrological responses during wet and dry seasons can be reproduced by using different parameter sets in the PDM. Our research objective is to configure the season-based PDM for southeastern Brazilian basins with size up to ~70,000 km^2 and obtain the optimal subannual PDM hydrological simulations for runoff forecasting and prediction for five important southeastern Brazilian basins (Figure 1). For the sake of simplicity, the basins are named in the paper by the respective upstream reservoir as Cantareira (2,279 km^2), Emborcação (29,076 km^2), Três Marias (51,576 km^2), Furnas (52,197 km^2), and Mascarenhas (71,649 km^2). The study was carried out in the context of providing scientific support for the critical water crisis that occurred in 2014 and 2015 in southeastern Brazil. The Cantareira reservoir system is the main source of water supply for the metropolitan region of São Paulo; and Emborcação, Três Marias, Furnas, and Mascarenhas reservoirs are important for hydropower generation in Brazil along with other purposes such as irrigation and water supply. However, during 2014 and 2015, Cantareira reached its lowest volume over the last 35 years; from November 2014 to February 2015, the other basins reached their respective lowest values over the last 15 years. The useful volume was approximately −20% to 0% for Cantareira from June 2014 to December 2015 and was ~3–10% for Três Marias from July 2014 to January 2015. We selected the period 1985–2015 for study due to data availability. To achieve the objective, three model calibration configuration schemes are considered on the basis of previous studies of Bekele and Nicklow (2007), Zhang, Moreira, and Corte-Real (2016), Muleta (2012), Kim and Lee (2014), and Zhang et al. (2015). First, the PDM is automatically calibrated by using the genetic algorithm for multiple objective function optimization called the nondominated sorting genetic algorithm II (Deb, Pratap, Agarwal, & Meyarivan, 2002). We also test whether the automated calibration is satisfactory, or if there is also merit in performing some manual calibration. Second, the calibration is carried out with the objective of obtaining the best model performance for both high and low flows. Finally, different parameter settings are considered for the wet and dry periods of simulation, and seasonally dependent parameter settings are calibrated simultaneously (in series). The PDM parameters configured in this
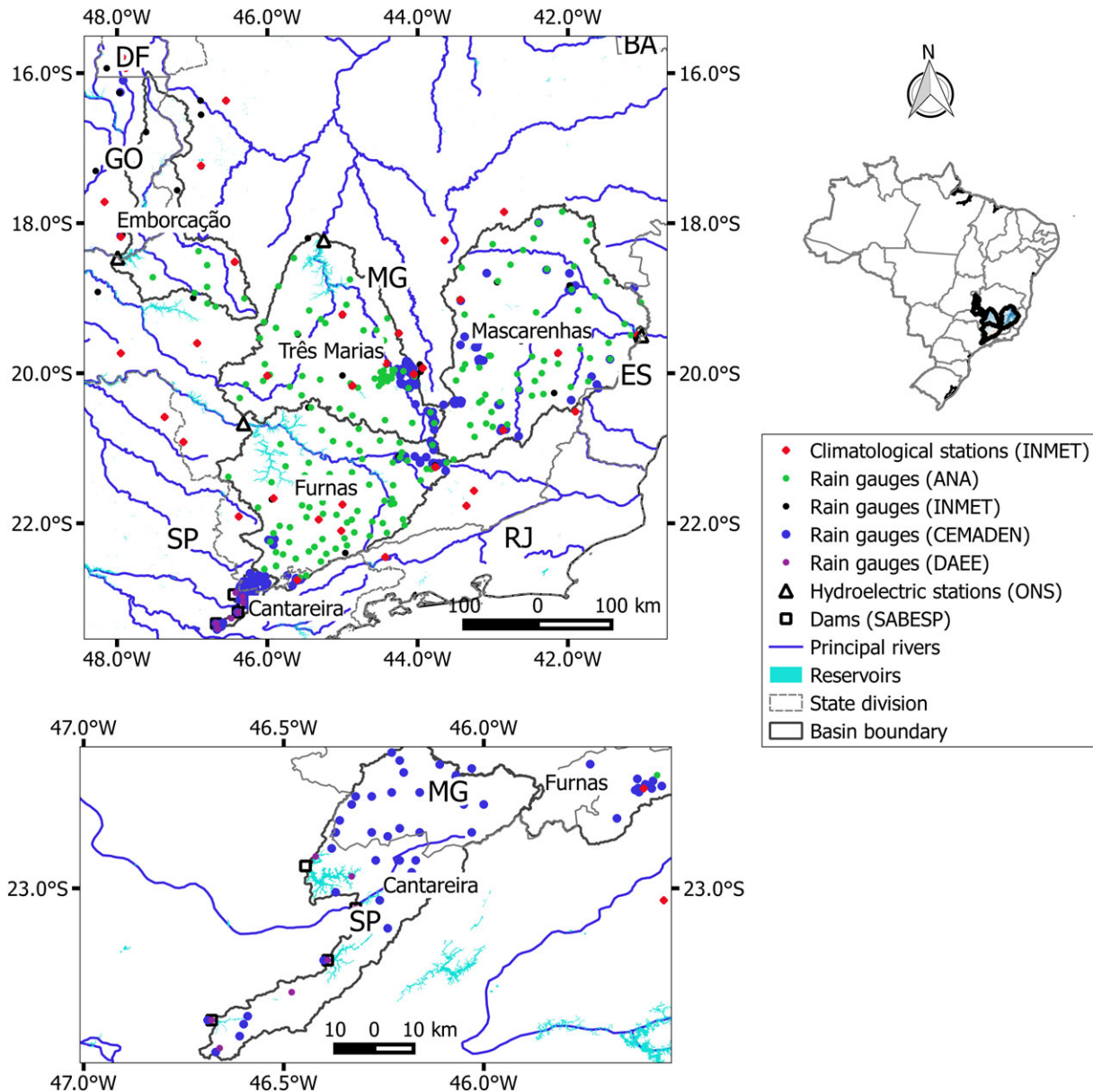
FIGURE 1 Map of location for the Cantareira, Emborcação, Três Marias, Furnas, and Mascarenhas basins in southeastern Brazil, showing the climatological stations from INMET (Brazilian National Institute of Meteorology); rain gauges from ANA (National Water Agency of Brazil), INMET, CEMADEN (Brazilian National Center for Monitoring and Early Warning of Natural Disasters), and DAEE (Brazilian Department of Water and Electric Energy); hydroelectric stations from ONS (Brazilian National Electric System Operator); dams from SABESP (São Paulo state water and waste management company); principal rivers; and reservoirs. BA, DF, ES, GO, MG, RJ, and SP represent states of Bahia, Distrito Federal, Espírito Santo, Goiás, Minas Gerais, Rio de Janeiro, and São Paulo

study are to be used in runoff forecasting and prediction for southeastern Brazilian large basins.

2 | DATA AND METHODS

2.1 | Study area and data

Figure 1 displays the location (16°S–24°S, 41°W–48°W) of the study area. Plateau and mountain are the main landforms; flood plains are also an important landform for Três Marias (43%) and Mascarenhas (17%). For Cantareira, Emborcação, Três Marias, Furnas and Mascarenhas, respectively, elevation varies in the ranges of 745–

2,027, 548–1,262, 561–1,546, 756–2,407, and 65–2,575; and the mean value is around 1,119, 883, 796, 1,002, and 608 m. The principal soil types are Oxisols, Inceptisols, and Ultisols (Figure S1 and Table S1); the main land use types are pasture, livestock and agriculture, and forest (Figure S2 and Table S2). The region is characterized by a humid subtropical climate with dry winters and hot summers, which has been classified as Cwa or Cwb by Peel, Finlayson, and McMahon (2007), with the classification details described by Alvares et al. (2013). Daily rainfall and PET are inputs to the PDM hydrological model. The precipitation and climatological stations' distribution are shown in Figure 1. Data source and availability period are shown in Table 1. For each climatological station, daily PET was calculated by the Hargreaves–Samani 1985 method (Hargreaves & Allen, 2003)

using daily maximum and minimum 2-m air temperature. For each basin, daily rainfall and PET were determined by the arithmetic mean of all available stations. Although other methods such as weighting for elevation or Thiessen polygons can be better alternatives, the arithmetic mean was used for its simplicity.

During the period 1985–2015, the average annual precipitation, PET, and runoff of the basins varied in the range of 1,200–1,500, 1,500–1,600, and 400–500 mm, respectively (Table 2). The flow variability was similar among them, but it was the smallest for Cantareira, Emborcação, and Furnas; largest for Três Marias; and second largest for Mascarenhas (Figure S3a–b). During 2005–2015, the mean daily discharge was ~1.3 mm/day for Cantareira, Emborcação, and Furnas; ~1.0 mm/day for Três Marias; and ~0.9 mm/day for Mascarenhas (Figure S3c).

2.2 | PDM-CEMADEN hydrological model

The PDM is a lumped rainfall–runoff model, transforming catchment-scale rainfall and PET into flow at the catchment outlet (Moore, 1985; Moore, 2007; Moore & Bell, 2002). Apart from a small handling charge, PDM (Moore, 2007) is available for free for academic educational use. However, due to its nonfree access for commercial use, Cuartas (2008) developed the PDM-CEMADEN model based on the PDM of Moore and Bell (2002) and Moore (2007). In this study, PDM-CEMADEN was operated at a daily time step; it reproduced hydrological processes by considering the following: (a) Actual evapotranspiration (AET) as the product of the Hargreaves–Samani 1985 PET and percentage of available soil moisture storage capacity (Equation 8 in Moore, 2007). The AET/PET was set to be linearly related to

the soil moisture deficit, $\frac{AET}{PET} = 1 - \left\{ \frac{(S_{max} - S(t))}{S_{max}} \right\}$, where $S(t)$ is

available soil moisture and S_{max} is soil moisture storage capacity; (b) soil moisture storage of a soil column at any point within a river basin represented by a Pareto distribution (Moore, 2007); (c) groundwater recharge, which is linearly related to the available soil moisture content and routed through a subsurface storage by using a cubic storage reservoir specified by the Horton–Izzard equation (Dooge, 1973). A recursive solution scheme of the subsurface storage was obtained by applying the approximate solution provided by Smith (1977); (d) direct runoff, which is derived from the principle of conservation of mass involving rainfall, AET, groundwater discharge, change of soil moisture storage, and direct runoff and routed through surface storage by using a cascade of two linear reservoirs (O'Connor, 1982).

2.3 | Seasonal calibration

2.3.1 | Seasonality

Quantitatively, the intra-annual variability of rainfall was measured by the rainfall seasonality index (SI; Walsh & Lawler, 1981), precipitation concentration index (PCI; Oliver, 1980), and modified Fournier index (MFI; Arnoldus, Boodt, & Gabriels, 1980; Fournier, 1960), such that

$$SI_i = \Sigma_{j=1}^{12} \left| \frac{X_{ij} - \overline{X_i}}{12\overline{X_i}} \right| , \tag{1}$$

$$PCI_i = 100 \times \Sigma_{j=1}^{12} \left[\frac{X_{ij}^2}{\left(\Sigma_{j=1}^{12} X_{ij} \right)^2} \right] , \tag{2}$$

$$MFI_i = \Sigma_{j=1}^{12} \left(\frac{X_{ij}^2}{\Sigma_{j=1}^{12} X_{ij}} \right) , \tag{3}$$

TABLE 2 The observed annual mass-balance components of the study area

Statistics[a]	Precipitation (mm/year)	Runoff (mm/year)	PET (mm/year)	Runoff coefficient (%)	CV (−)
Emborcação	1,469	475	1,620	32	0.16
Três Marias	1,386	383	1,605	28	0.16
Furnas	1,458	512	1,558	35	0.13
Mascarenhas	1,219	374	1,535	31	0.19

Note. CV = coefficient of variation showing interannual variability of precipitation.

[a]The statistics are derived from the observation during the period 1985–2015.

where X is the mean daily precipitation; the subscripts i and j are the year and month of the examined precipitation; and $\overline{X_i}$ is the mean value over the year i.

The intra-annual and interannual variability of rainfall was evaluated by the coefficient of variation (CV; Dingman, 2015), defined as

$$CV_i = \sqrt{\frac{1}{12-1}\sum_{j=1}^{12}\left(\frac{X_{ij}-\overline{X_i}}{\overline{X_i}}\right)^2} \tag{4}$$

$$CV = \sqrt{\frac{1}{n-1}\sum_{i=1}^{n}\left(\frac{\overline{X_i}-\overline{X}}{\overline{X}}\right)^2} \tag{5}$$

where CV_i is the intra-annual variability of the year i, CV is the interannual variability over the n years, and $\overline{X}$ is the mean daily precipitation over the n years.

A year was considered seasonal if there was a dry season, and markedly seasonal when there was a long dry season (Table S3). Seasonal years were defined to have SI in the range of 0.60–0.79, PCI of 15–20, and CV of 0.80–0.99; markedly seasonal years have SI in the range of 0.80–0.99, PCI of 20–50, and CV of 1.00–1.19. Rainfall erosivity was considered high if MFI was in the range of 120–160 and very high when MFI was larger than 160. Larger CV, SI, PCI, and MFI indicate larger rainfall variability. CV expresses the extent of variability in relation to the mean. SI, PCI, and MFI measure the distance of observed rainfall from uniform distribution. MFI evaluates the effect of erosion by rainwater: Higher (lower) values indicate larger (smaller) rainfall erosivity.

2.3.2 | Seasonal calibration of the PDM-CEMADEN model

According to Moore (2007), Cabus (2008), and Vleeschouwer and Pauwels (2013), the calibration parameters of PDM-CEMADEN were selected as follows: maximum (c_{max}) and minimum (c_{min}) soil moisture storage capacity, exponent of Pareto distribution controlling spatial variability of storage capacity (b), and time constants of groundwater recharge (k_g), baseflow (k_b), and two linear reservoirs (k_1 and k_2). Other parameters were set as follows: Exponent of the AET function (b_e) was set to 1, exponent of the recharge function (b_g) was 1, and exponent of the baseflow non-linear storage (m) was 3; soil tension storage capacity (S_t) was set to 0.45 times total available storage S_{max}, initial

soil moisture storage ($S(t)_{ini}$) was set to 1.25 times S_t, and initial groundwater storage ($S_g(t)_{ini}$) was set to 6.0 mm; constant of flow addition (q_c) was set to 0 m^3/s.

The indicators SI, PCI, MFI, and CV were not used for the definition of wet and dry seasons because they only reflect the seasonality of rainfall and so do not include the influences of soil and other climatic conditions of a catchment. Like Muleta (2012), this study used a monthly runoff coefficient to separate wet and dry seasons. The runoff coefficient was defined as the ratio of total runoff at the basin outlet to the total rainfall. For each month, the ratio to mean of the runoff coefficient was derived from the ratio of the climatological mean of runoff coefficient over the month to that over the entire year. A year was divided into wet, dry, and transitional seasons, which had the ratio to mean values of >1.0, <1.0, and ~1.0, respectively. Different model parameter settings were assumed for each season, and they changed linearly from one to another season. Table 3 displays the parameter ranges for the five basins. The nondominated sorting genetic algorithm II method (Deb et al., 2002) with the configuration recommended by Zhang et al. (2016) was applied for automatic calibration of PDM-CEMADEN; and the package "DEAP 1.1.0" written in the Python programming language (http://deap.gel.ulaval.ca/doc/dev/) was used to implement the optimization. Each optimization was repeated 30 times to consider the random seed effects. The automatic calibration intended to maximize both the Nash–Sutcliffe efficiency (NSE; Nash & Sutcliffe, 1970) and the logarithmic transform (NSElog; Krause, Boyle, & Bäse, 2005) for wet, dry, and transitional seasons, defined as

$$NSE = 1-\frac{\sum_{i=1}^{n}[Q_o(i)-Q_s(i)]^2}{\sum_{i=1}^{n}[Q_o(i)-\overline{Q_o}]^2} \tag{6}$$

$$NSElog = 1-\frac{\sum_{i=1}^{n}[\log_{10}(Q_o(i))-\log_{10}(Q_s(i))]^2}{\sum_{i=1}^{n}[\log_{10}(Q_o(i))-\log_{10}(\overline{Q_o})]^2} \tag{7}$$

where Q_o and Q_s represent the observed and simulated daily mean discharges at basin outlet, respectively; n is the number of days; and $\overline{Q_o}$ is the mean observed daily discharge. According to Moriasi et al. (2007), model performances can be judged as very good if both NSE and NSElog are in the range of 0.75–1.00, good if the values are in 0.65–0.75, and satisfactory if they are in 0.50–0.65.

TABLE 3 Parameter settings of the PDM-CEMADEN hydrological simulations

Parameters[a]		C_{max} (mm)	C_{min} (mm)	b (–)	k_g (days)	k_b (days·m^2)	k_1 (days)	k_2 (days)
Cantareira	Max	200	60	0.10	100	1,000	0.01	0.01
	Min	2,700	170	1.50	1,000	5,000	5.00	5.00
Emborcação	Max	200	60	0.10	100	1,000	1.00	1.00
	Min	2,700	170	1.50	1,000	5,000	30.00	30.00
Três Marias	Max	200	60	0.10	100	1,000	1.00	1.00
	Min	2,700	170	1.50	1,000	5,000	30.00	30.00
Furnas	Max	200	60	0.10	100	1,000	1.00	1.00
	Min	2,700	170	1.50	1,000	5,000	30.00	30.00
Mascarenhas	Max	200	60	0.10	100	1,000	1.00	1.00
	Min	2,700	170	2.00	1,000	5,000	50.00	50.00

Note. Max = maximum; Min = minimum.

[a]These parameter ranges apply to both seasonal and traditional calibrations.

For Cantareira, PDM-CEMADEN was calibrated for the period from October 1, 2005, to September 30, 2010, and validated from October 1, 2010, to January 20, 2016. For Emborcação, Três Marias, Furnas, and Mascarenhas, the validation period was split into two, in which the second period represents a dry period, to test the capacity of PDM-CEMADEN in reproducing hydrological processes under such conditions. The calibration was from October 1, 1984, to September 30, 2001, for Emborcação, Três Marias, and Furnas and from October 1, 1986, to September 30, 2001 for Mascarenhas; the validation was from October 1, 2001, to September 30, 2010, and then from October 1, 2010, to the end of data availability.

3 | RESULTS AND DISCUSSION

3.1 | Hydrological seasonality of southeastern Brazil

We found distinct seasonality in rainfall, runoff, and runoff coefficient for the study area under mean climate of 1985–2015 (Figures 2 and S4). The mean rainfall divides a year into four parts: (a) January and

December; (b) February, March, and November; (c) October; and (d) April to September. And each division has respective monthly rainfall of ~2.5, ~1.5, ~0.8, and ~0.3 times the mean climatological annual total. Monthly runoff has a similar pattern of variation as rainfall but with a lag of 1 month. The mean runoff partitions a year into three parts: (a) January, February, March, and December; (b) April and November; and (c) May to October. And each division has a respective monthly runoff of ~2.0, ~1.0, and ~0.5 times the mean climatological annual total. Compared with rainfall and runoff, monthly PET varies moderately, in the range of 0.7–1.2 times the climatological mean, throughout a year. On the basis of the runoff coefficient values, we divided a year into (a) October to February as the wet period, (b) March and September as the transitional period, and (c) April to August as the dry period, for hydrological simulations using the PDM-CEMADEN model.

We classified the study area as seasonal in normal years and highly seasonal in occasional years. The SI mainly varies in the range of 0.6–0.8 and sometimes between 0.8 and 1.0 (Figure 3a), which indicates the precipitation regime is mainly seasonal and sometimes markedly seasonal with a long dry season according to Walsh and Lawler
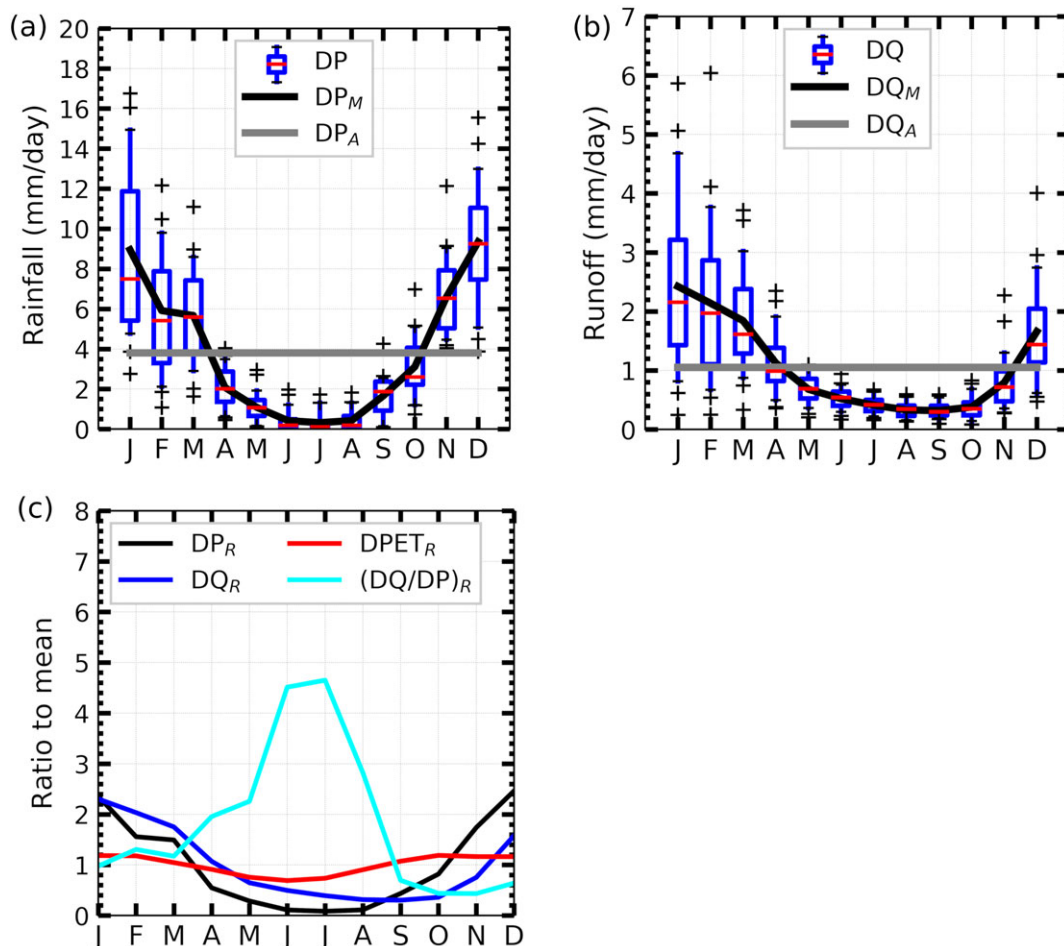

FIGURE 2 Plots of annual cycles of (a) mean daily rainfall DP and (b) runoff DQ for the Três Marias basin; plot (c) represents the river regime by monthly ratio to mean of daily rainfall DPR, runoff DQR, runoff coefficient (DQ/DP) R, and potential evapotranspiration DPETR. In plots (a)–(b), the boxplots show the monthly variation of DP and DQ during the period 1985–2015; the bold black line displays the climatological mean (DPM or DQM) over the month; and the bold grey line shows the climatological mean over the entire year (DPA or DQA). For each boxplot, the lower and upper whiskers represent the 5th and 95th percentiles, and the bottom and top of the box display the 25th and 75th percentiles, respectively. The line inside the boxplot shows the 50th percentile. In plot (c), the ratio to mean for a specified month is defined as the ratio of the climatological mean of daily value over the month to that over the entire year
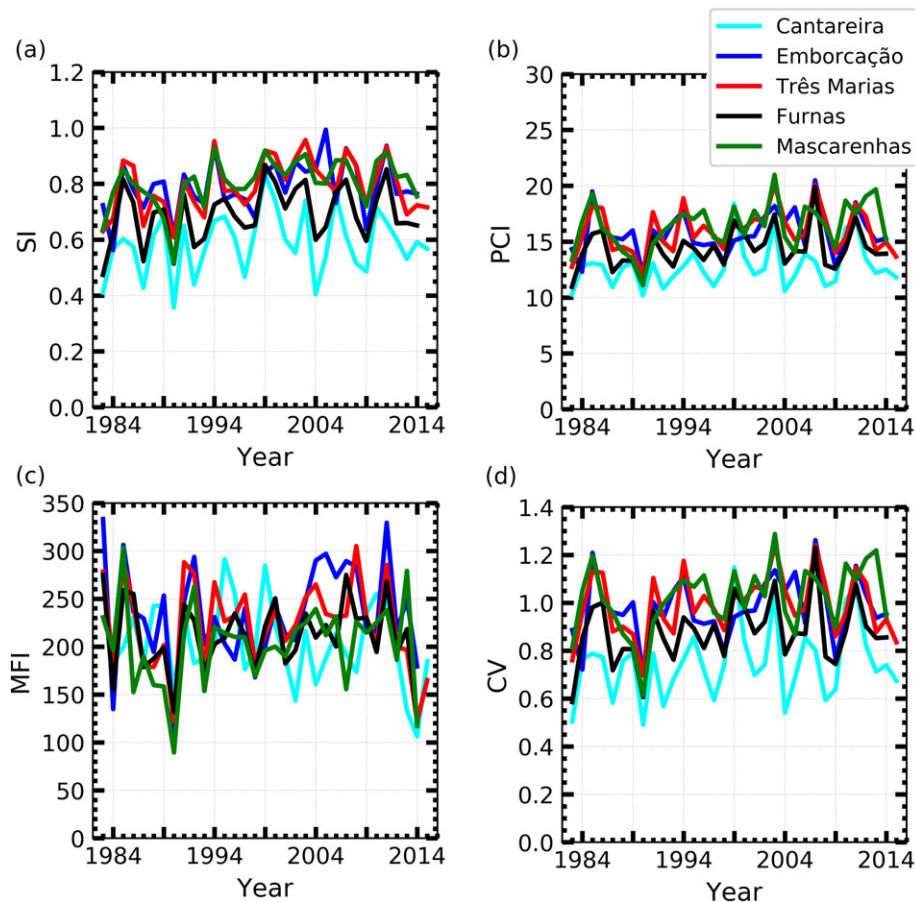
FIGURE 3 Plots of the (a) seasonality index (SI), (b) precipitation concentration index (PCI), (c) modified Fournier index (MFI), and (d) coefficient of variation (CV) during the period 1983–2015

(1981; Table S3a). The PCI mostly varies in the range of 15–20 and occasionally between 10 and 15 (Figure 3b), which means that the precipitation concentration is mostly seasonal and occasionally moderately seasonal according to Oliver (1980; Table S3b). The MFI mainly varies between 160 and 260 except for the years 1990 and 2014 (Figure 3c).

Overall, the intra-annual variability of hydrological variables is larger than the interannual variability, and seasonality of the five study basins is characteristic of a Mediterranean climate. The CV is of ~0.8–1.1 (Figure 3d and Table S4) and ~0.16 (Table 2) for intra-annual and interannual rainfall variability, respectively. On the basis of the data from land gauge precipitation records of the Global Historical Climatology Network, Version 2, and reanalysis, Fatichi, Ivanov, and Caporali (2012) found that CV ranges from 0.1 to 0.6 for interannual variability of precipitation at global scale, and it is ~0.1, which is relatively small, for southeastern Brazil. For the monthly climatological rainfall, for Cantareira, Emborcação, Três Marias, Furnas and Mascarenhas, respectively, the SI is ~0.5, ~0.7, ~0.7, ~0.6, and ~0.6; the PCI is 11.3, 14.1, 14.3, 13.0, and 14.2; and the MFI is 173.9, 202.0, 192.5, 185.1, and 168.3. These values are comparable or higher than those obtained by García-Marín, Ayuso-Mu oz, Cantero, and Ayuso-Ruiz (2017) for western Andalusia, which is in a Mediterranean climate region with a high potential risk of soil erosion by rainfall, during the period 1945–2005. The SI of the study area is comparable with that of western Andalusia (~0.3–0.8, Figure 5b in García-Marín et al.,

2017); the PCI is larger than most parts of western Andalusia (~10.0–14.0, Figure 7b in García-Marín et al., 2017); and the MFI is larger than that of western Andalusia (~60~160, Figure 10b in García-Marín et al., 2017). Due to the characteristics of the precipitation being seasonal and with large totals, southeastern Brazil, compared with other regions of the world, has a large rainfall erosivity (Table S3c). Nevertheless, the erosivity is much smaller than that of the Amazon region (Figure 2b in da Silva, 2004). The larger intra-annual variability, compared with the interannual variability, justifies the partition of the study period into wet, dry, and transitional seasons according to the monthly runoff coefficient values. The seasonality is similar among the basins, although Furnas and Cantareira have a smaller seasonality than the others. Therefore, we used the same division of seasons for hydrological simulation of the five basins. The classification methodology is in accordance with Muleta (2012).

3.2 | Calibration and validation

Considering different parameter setting for each season, the PDM-CEMADEN model was successfully calibrated and validated for the five study basins. This is demonstrated in Figure 4 by performance indicators NSE and NSElog for the nondominated solutions, which were obtained by the optimization process of the model calibration. The nondominated solutions are equally good; neither NSE nor NSElog can be improved in value without degrading the other
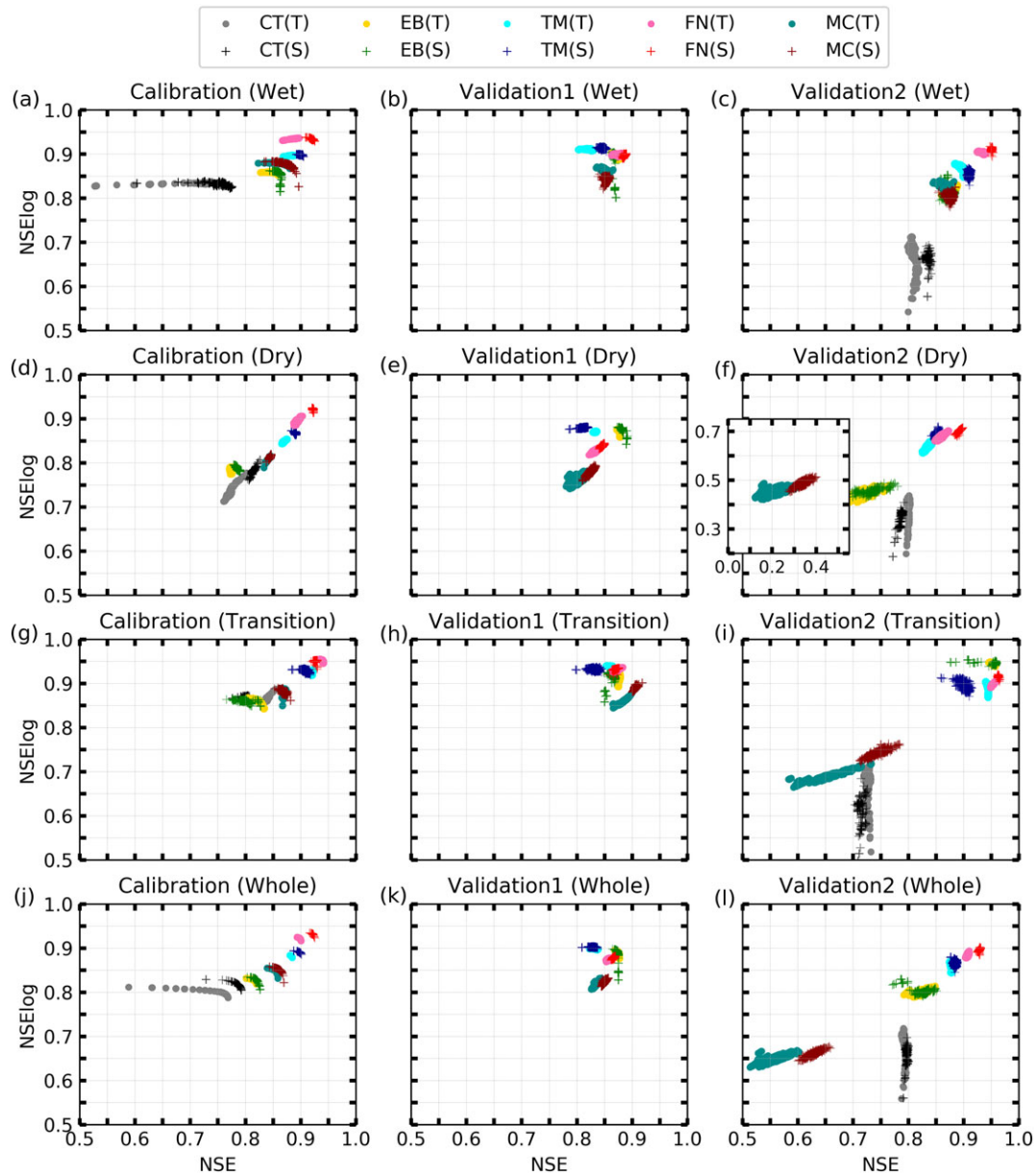
FIGURE 4 (a)–(l) Plots of PDM-CEMADEN performance for simulating the daily mean discharges at outlets of the Cantareira (CT), Emborcação (EB), Três Marias (TM), Furnas (FN), and Mascarenhas (MC) basins. T and S represent traditional and seasonal calibration of the PDM-CEMADEN model. NSE and NSElog represent Nash–Sutcliffe efficiency and logarithmic Nash–Sutcliffe efficiency. The wet season is October to February; the dry season is April to August; the transitional season is March and September. (f) The small window zooms in on the performance points located outside the plot window

objective value. Solutions, which are located at the upper and right parts of each plot, are the preferable ones. For the calibration period (Figure 4a, d, g, and j), the results for the seasonal calibration of the PDM-CEMADEN model are very good for all the five basins. The nondominated solutions reproduced daily mean discharges at the basin outlet not only during the wet, dry, and transitional seasons separately but also during the whole period. For the whole calibration period, NSE and NSElog of the optimal solutions are ~0.92 and ~0.92 for Furnas, ~0.90 and ~0.90 for Três Marias, ~0.87 and ~0.86 for Mascarenhas, ~0.83 and ~0.83 for Emborcação, and ~0.78 and ~0.82 for Cantareira, respectively. For the validation period 2001–2010 (Figure 4b, e, h, and k), the results for the seasonal calibration are very good for Furnas, Três Marias, Mascarenhas, and Emborcação. For the whole validation period 2001–2010, NSE and NSElog of the

optimal solutions are ~0.87 and ~0.87 for Furnas, ~0.84 and ~0.90 for Três Marias, ~0.85 and ~0.83 for Mascarenhas, and ~0.87 and ~0.90 for Emborcação, respectively. For the validation period 2010–2015 (Figure 4c, f, i, and l), the results for the seasonal calibration are very good for Furnas, Três Marias, and Emborcação; good for Cantareira; and satisfactory for Mascarenhas. For the whole validation period 2010–2015, NSE and NSElog of the optimal solutions are ~0.93 and ~0.90 for Furnas, ~0.88 and ~0.87 for Três Marias, ~0.85 and ~0.81 for Emborcação, ~0.80 and ~0.70 for Cantareira, and ~0.66 and ~0.68 for Mascarenhas, respectively.

The season-based PDM-CEMADEN model was capable of reproducing hydrological processes under both wet and dry conditions, which is demonstrated by the very good model performances for Furnas and Três Marias during the calibration and validation periods

(Figure 4). Overall, for the five study basins, PDM-CEMADEN performed better for the wet season than for the dry season; and for both wet and dry seasons, the performances for high flows are better than those for low flows. The model performed less well for Emborcação, Cantareira, and Mascarenhas, compared with Furnas and Três Marias, and the performance differences are larger for the dry period from 2010 to 2015. Throughout the full period 2010–2015, PDM-CEMADEN performed less well in reproducing low flows at the outlet of Cantareira; during the dry season of 2010–2015, the model performed less well for Emborcação and Mascarenhas. This may be a result of a problem with PET estimates from the three basins. Due to a lack of data availability, the daily PET of Cantareira was derived from nearby meteorological stations located outside the drainage area, which has inevitably caused uncertainties in the estimation of daily AET; for Emborcação and Mascarenhas, the data quality problem may be associated with the sparse location of the climatological stations. During the dry period or particularly low flow period, the uncertainties of PET may be a dominant cause of the modelling errors because AET is the main water flux in the daily water balance (Samain & Pauwels, 2013).

The successful calibration and validation of PDM-CEMADEN is also indicated in Figures 5, 6, S5, and S6 by displaying the capacity of the selected optimal solution in reproducing annual, seasonal, daily, and monthly mean discharges at the basin outlet. For the whole of the calibration period, NSE and NSElog values are 0.79 and 0.81 for Cantareira, 0.81 and 0.83 for Emborcação, 0.90 and 0.89 for Três Marias, 0.92 and 0.93 for Furnas, and 0.85 and 0.86 for Mascarenhas (Tables 4 and 5), respectively. The selected optimal solutions have reproduced well the annual (Figure 5a), seasonal (Figure 5b), daily (Figures 6 and S5), and monthly (Figure S6) discharges at the outlets of the five study basins, for both the calibration and validation periods. Overall, the model performances are considered very satisfactory according to Moriasi et al. (2007). At the annual scale, errors of the simulated runoff, at interquartile ranges and a probability level between 5%

and 95%, are in the ranges of approximately −10% to 15% and approximately −22% to 30%, respectively; during the wet season, the errors are in the ranges of approximately −12% to 18% and approximately −25% to 25%, respectively; during the dry season, they are in the respective ranges of approximately −11% to 22% and approximately −20% to 39%; and during the transitional season, they are in the respective ranges of approximately −21% to 14% and approximately −24% to 42%. Extreme errors in the simulated runoff are mainly in years with less precipitation (Figure 5b). The error of simulated annual runoff for the hydrological year 2013/2014 for Cantareira, Três Marias, and Furnas is approximately −21%, ~22%, and ~22%, respectively; the error for 1986/1987 and 1994/1995 for Emborcação is ~30% and approximately −28%, respectively; the error for 2014/2015 for Mascarenhas is ~46%. As displayed in Figure 4, the model performed less well in the simulation of the dry or low flow period. This is evident for Cantareira (Figures S5(1) b and S6(1)b), Emborcação (Figures S5(2) a, c, and S6(2) a, c) and Mascarenhas (Figures S5(4)b–c and S6(5)b–c) by comparing the observed and simulated discharges. In addition, underestimations of peak discharges are also identified (Figures 6 and S5), which are particularly obvious for Três Marias (Figure 6b) and Mascarenhas (Figure S5(4)a–c). Further studies are required for clarification.

3.3 | Seasonal versus traditional calibration

To illustrate the effect of seasonal calibration, PDM-CEMADEN was also calibrated considering a unique set of parameters throughout the simulation period (traditional calibration). The nondominated solutions from the seasonal and traditional calibrations were compared in terms of performance indicators NSE and NSElog (Figure 4). The selected optimal solutions for the two calibrations were also compared in terms of reproducing monthly and daily mean discharges at basin outlet (Figures 6 and S5–S8). We found that, in general, the seasonal calibration produced better results than did the traditional calibration
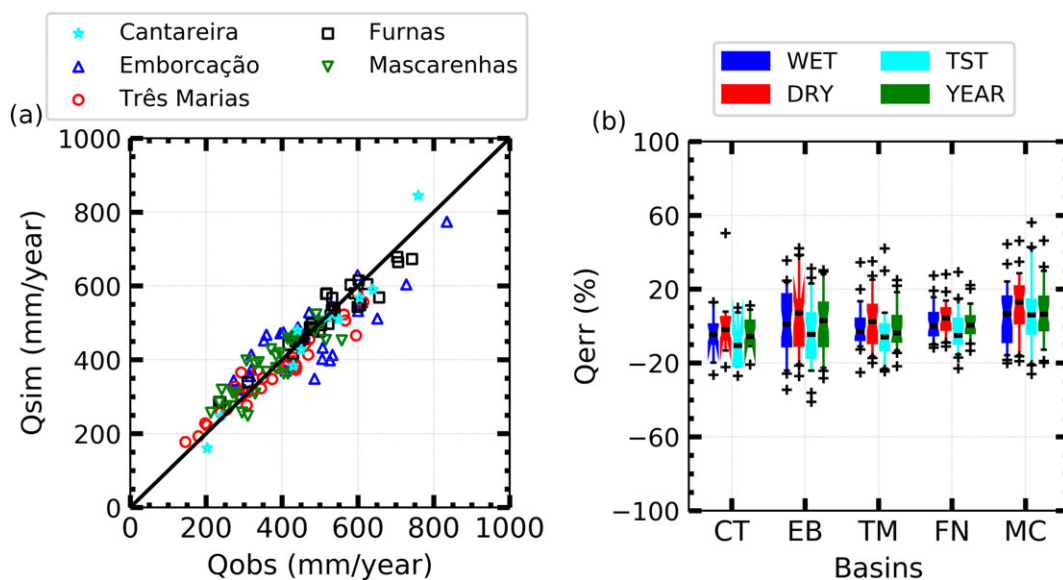

FIGURE 5 Plots for evaluating the PDM-CEMADEN performance in reproducing annual and seasonal runoffs: (a) Scatter plot showing the comparisons between the observed (Qobs) and simulated (Qsim) daily mean discharges at basins outlet; (b) boxplots showing errors (Qerr) of the simulated discharges during the wet, dry, and transitional (TST) seasons and the entire year
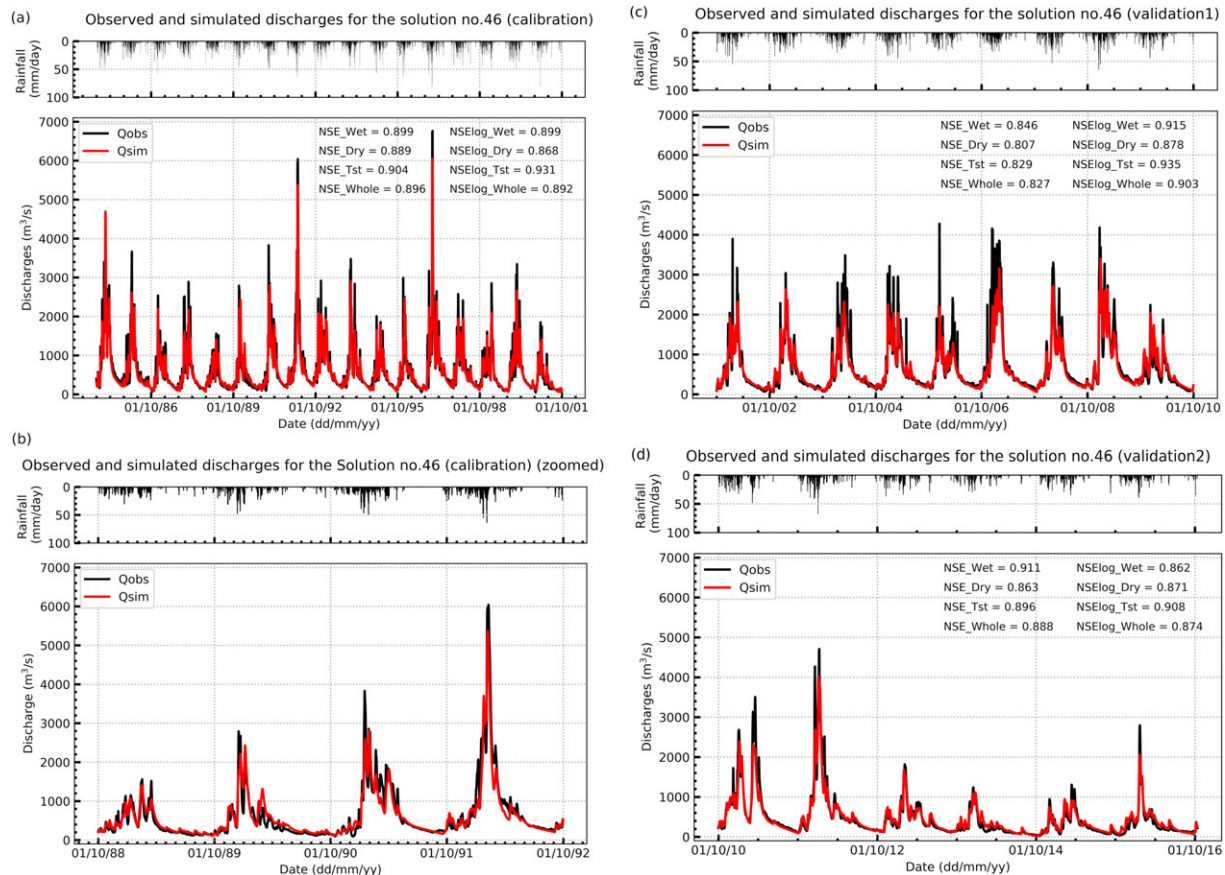
FIGURE 6 Plots for comparison of the simulated and observed daily discharges for the Três Marias basin (seasonal calibration) during the periods (a) from October 1, 1984, to September 30, 2001; (b) from October 1, 1988, to September 30, 1992; (c) from October 1, 2001, to September 30, 2010; and (d) from October 1, 2010, to October 12, 2016. (b) A zoomed-in hydrograph of (a)

TABLE 4 Optimal parameter settings of the PDM-CEMADEN hydrological simulations (seasonal calibration)

Parameters[a]		C_{max} (mm)	C_{min} (mm)	b (−)	k_g (days)	k_b (days·m^2)	k_1 (days)	k_2 (days)
Cantareira	Wet	1,784.5	85.5	0.27	342.3	1,202.3	0.01	3.18
	Dry	1,541.0	169.7	0.17	428.6	1,042.5	0.01	2.44
Emborcação	Wet	2,168.3	169.7	0.30	428.3	4,871.7	1.01	6.72
	Dry	2,117.6	168.1	0.29	528.2	4,937.1	1.00	9.95
Três Marias	Wet	1,548.4	168.3	0.34	731.4	4,912.3	1.00	9.13
	Dry	1,434.6	169.8	0.22	739.3	4,660.1	1.00	11.28
Furnas	Wet	2,028.1	170.0	0.57	423.6	4,703.0	1.80	7.12
	Dry	1,431.2	169.3	0.23	479.8	4,980.6	1.02	8.93
Mascarenhas	Wet	2,699.6	165.6	0.34	573.6	4,197.1	1.50	5.27
	Dry	2,637.7	161.6	0.31	676.6	4,994.0	1.27	7.30

Note.

[a]The wet and dry periods are defined on the basis of their runoff coefficients; the wet season is October to February; and the dry season is April to August.

for the wet, dry, transitional, and whole periods of both calibration and validation periods. The performance differences are mainly in NSE for the wet period, and NSE and NSElog for the dry period. This means that the seasonal calibration has improved model performance in high flow simulation for the wet period, and both high and low flow simulation for the dry period. The results indicate that seasonally dependent parameter settings can be used in PDM rainfall–runoff modelling for the simulation of hydrological processes during different seasons. Together with input variables of rainfall and PET, seasonally dependent parameter settings are used to capture the seasonal

behaviours in a more realistic way. Their use reproduces the influences of seasonality on physical processes such as infiltration, surface water flow, subsurface water flow, and baseflow. This is not the case for the use of seasonally independent parameter setting by traditional calibration, as only the input variables are used to consider the seasonal behaviours. The use of seasonally independent parameter settings may produce inaccurate or erroneous soil moisture conditions and runoff as initial conditions of a hydrological forecast or prediction. Therefore, seasonal calibration provides a better preparation of the PDM than does traditional calibration for the purpose of hydrological

TABLE 5 Performance of the optimal PDM-CEMADEN hydrological simulations

Performance indicators[a,b]		CT	EB	TM	FN	MC
Calibration	NSE_{WET}	0.76	0.85	0.90	0.92	0.86
	$NSElog_{WET}$	0.83	0.86	0.90	0.94	0.88
	NSE_{DRY}	0.81	0.78	0.89	0.92	0.85
	$NSElog_{DRY}$	0.78	0.80	0.87	0.92	0.82
	NSE_{TST}	0.80	0.78	0.90	0.92	0.86
	$NSElog_{TST}$	0.87	0.86	0.93	0.95	0.89
	NSE_{WHOLE}	0.79	0.81	0.90	0.92	0.85
	$NSElog_{WHOLE}$	0.81	0.83	0.89	0.93	0.86
Validation1	NSE_{WET}		0.87	0.85	0.89	0.85
	$NSElog_{WET}$		0.90	0.92	0.90	0.85
	NSE_{DRY}		0.88	0.81	0.85	0.83
	$NSElog_{DRY}$		0.88	0.88	0.84	0.79
	NSE_{TST}		0.86	0.83	0.87	0.91
	$NSElog_{TST}$		0.92	0.94	0.93	0.90
	NSE_{WHOLE}		0.87	0.83	0.87	0.85
	$NSElog_{WHOLE}$		0.90	0.90	0.88	0.83
Validation2	NSE_{WET}	0.84	0.89	0.91	0.95	0.87
	$NSElog_{WET}$	0.67	0.81	0.86	0.92	0.81
	NSE_{DRY}	0.79	0.77	0.86	0.90	0.40
	$NSElog_{DRY}$	0.69	0.75	0.87	0.88	0.51
	NSE_{TST}	0.72	0.96	0.90	0.96	0.78
	$NSElog_{TST}$	0.64	0.95	0.91	0.92	0.76
	NSE_{WHOLE}	0.80	0.85	0.89	0.93	0.66
	$NSElog_{WHOLE}$	0.67	0.81	0.87	0.90	0.68

Note.

[a]The performance indicators were calculated from comparisons between observed and simulated daily discharges at the outlet of the Cantareira (CT), Emborcação (EB), Três Marias (TM), Furnas (FN), and Mascarenhas (MC) basins.

[b]NSE is the Nash–Sutcliffe efficiency and NSElog is the logarithmic Nash–Sutcliffe efficiency. The subscripts WET, DRY, TST, and WHOLE mean that the evaluation of performance indicators are carried out only for the wet, dry, transitional, and whole periods, respectively. The definitions of wet, dry, and transitional periods can be found in Figure 4, and the calibration and validation periods can be found in Section 2.3.

forecasting and prediction. The added complexity of seasonal calibration relative to traditional calibration is well justified. Also, the division of seasons by the mean climatological monthly runoff coefficient makes possible the consideration of the overall influence from a combination of factors, such as soil, land cover, elevation, and mean climatological condition, on rainfall–runoff processes. The seasonal calibration of this study is the first attempt at capturing seasonal behaviours of hydrological process using seasonally dependent PDM parameters. Due to the data availability, seasonal changes in land use and vegetation were not explicitly included in the PDM hydrological simulation. And the AET estimation was simplified by using the same linear relation between AET/PET and soil moisture deficit for different seasons. Therefore, further improvements may be expected by taking a better account of evapotranspiration, considering its importance in the water balance of humid regions (Samain & Pauwels, 2013). For example, different relations between AET/PET and soil moisture deficit can be assigned by using different values of b_e, for different seasons; and seasonal changes in land use and vegetation can be included, in form of the leaf area index (LAI), in the rainfall–runoff modelling. Further investigations are required for clarifying how seasonal changes in land use and vegetation impact evapotranspiration as a function of weather variables and soil moisture (Brown, Zhang, McMahon, Western, & Vertessy, 2005).

3.4 | Model parameter analysis

The calibrated parameter settings are shown in Table 4 for the wet and dry seasons of the five basins. The parameters c_{max}, b, k_g, and k_2 are

seasonally different, although the differences vary among basins. Except for the value of k_2 in the Cantareira basin, the c_{max} and b (k_g and k_2) values during the wet season are larger (smaller) than those during the dry season. This means that during the wet season, the basin has a larger capacity and variation of soil water storage, larger soil water conductivity, and quicker surface water flow. During the wet season, rainfalls generally have larger amounts, higher intensity, longer duration, and higher frequency, which facilitate the occurrences of wetter soil moisture conditions, higher depth of surface water flow, and consequently larger soil water conductivity and quicker surface water flow; and the spatial heterogeneity in soil property, land cover, elevation, and climate promotes the larger variation of soil water storage. In addition, land cover in the wet season has a different LAI relative to dry season, which further influences the effective rainfall, infiltration rate, and soil water storage. Model parameters of different seasons may be different in order to produce the appropriate nonstationary climate and land use conditions. Comparing the seasonal difference of parameters among basins, we found that the differences of c_{max} and $b(k_g)$ are smaller for Emborcação and Mascarenhas (Três Marias). The differences of k_2 for Cantareira from the others may be explained by the parameter adjustment resulting from the deficiencies of rainfall and PET input. The seasonal calibration parameters (Table 4) are consistent or comparable with those obtained from previous studies. Cabus (2008) configured PDM for the 443.5-km² Grote Nete catchment with c_{max}, c_{min}, b, k_g, k_b, k_1, and k_2 of 1,000 mm, 70 mm, 0.75, 366.7 days, 2,400 days·mm², 0.58 days, and 1.67 days, respectively; Samain and Pauwels (2013) set PDM for the 88.4-km² Bellebeek catchment with c_{max}, c_{min}, b, k_g, k_b, k_1, and k_2 of 400 mm,

0 mm, 0.3, 215.6 days, 1.3 days·mm^2, 0.17 days, and 0.42 days, respectively. This study obtained seasonal c_{max} in the range of 1,431.2–2,699.6 mm for the five basins with areas in the range of 2,279–71,649 km^2. The larger soil moisture storage capacities than those of Grote Nete and Bellebeek may be explained by the larger area and different properties of soil and land use of the five basins. Grote Nete is characterized by sandy soil, which holds less water than other soil textures. The study area is dominated by soil types (for example, Oxisol) with substantial clay content, which can hold large soil water content even at wilting point (Tomasella, Hodnett, & Rossato, 2000). Bellebeek land use is dominated by agriculture (64%) and pasture (23%), whereas the five study basins are dominated by pasture (~40%), agriculture (~25%), and forest (~10%). The land use of Bellebeek may enable less field capacity than that of the study basins. The seasonal k_g is in the range of 342.3–739.3 days, which is comparable with that of Grote Nete and Bellebeek. For the Pareto distribution of storage capacity, the total storage capacity of the basin, $S_{max} = (bc_{min} + c_{max})/(b + 1)$, is in the range of 1,195.2–2,056.6 mm for the study basins, which is larger than that of Grote Nete (611 mm) and Bellebeek (308 mm). The seasonal k_2 of the study basins is in the range of 2.44–11.28 days, which is larger than that of Grote Nete and Bellebeek due to their larger runoff volume. For each basin, the parameters obtained from traditional calibration (Table S5) are located near or inside the ranges defined by the calibrated values for the wet and dry seasons. It implies that the traditional calibration results in parameters with values compromised to the varying seasonality. For example, c_{max} is 1,603.1 mm for the traditional calibration of Furnas, which is inside the range 1,431.2–2,028.1 mm, defined by the calibrated c_{max} for wet and dry seasons; k_b is 5,000 days·mm^2 for the traditional calibration of Furnas, and is near the range 4,703.0–4,980.6 days·mm^2, defined by the seasonal calibration. Furthermore, the total available storage (S_{max}) changes from 1,195.2 to 2,056.6 mm across the five basins and with season, which is comparable with 1,213.8 to 2,043.1 mm without seasons.

3.5 | PDM-CEMADEN and basin scales

This study applied the seasonal PDM-CEMADEN model to basins with areas up to 71,649 km^2, which is larger than previous PDM hydrological simulations (up to ~3,500 km^2) by Cabus (2008), Vleeschouwer and Pauwels (2013), and Bennett, Robertson, Ward, Hapuarachchi, and Wang (2016). In general, we found satisfactory results (Figures 4–6 and Table 5) for PDM-CEMADEN in reproducing hydrological processes of the study area, which confirms its potential use in hydrological forecasting and prediction for middle- and large-sized basins. We found different model performances for the five basins, of which the rank from high to low is Furnas, Três Marias, Emborcação, Cantareira, and Mascarenhas. Although there are scale differences among the study basins, conclusions about the relationship between model performance and basin scale cannot be established. It is not only due to the small number of samples but also because of the differences in the quality of input data. The PDM-CEMADEN simulations obtained better model performances for basins with better input data. For example, among the study basins, there are large differences in spatial heterogeneity of rain gauges and climatological stations' distribution.

The rain gauge distribution is not dense enough, particularly for Cantareira and Emborcação. Likewise, the climatological station distribution is not dense enough, particularly for Cantareira, Emborcação, and Mascarenhas. Overall, Furnas and Três Marias have better spatial distribution of rain gauges and climatological stations. Their better model performances have demonstrated the capacity of PDM-CEMADEN in reproducing seasonal hydrological processes in large-sized basins.

4 | CONCLUSIONS

This research made the first attempt at configuring different parameter settings of the PDM-CEMADEN model (Cuartas, 2008) for simulating different hydrological processes during wet and dry seasons. Considering the parameters c_{max}, c_{min}, b, k_g, k_b, k_1, and k_2 as seasonally dependent, the model successfully reproduced the intra-annual and interannual hydrological variability during the period 1985–2015 for five basins in southeastern Brazil with sizes up to ~70,000 km^2. The performances are very satisfactory not only during the wet, dry, and transitional seasons separately but also during the whole period. Overall, they are better for the wet season than for the dry season; and for both wet and dry seasons, the performances for high flows are better than those for low flows. The low performance for the dry season and low flows may be a result of data input quality problems with PET and the use of an inaccurate b_e value in AET estimation. The season-based PDM-CEMADEN model performed best for the Furnas basin (~50,000 km^2) where the input data of precipitation and PET are of the best quality.

Compared with the traditional PDM-CEMADEN model, the season-based model obtained better performance, because along with input variables of rainfall and PET, the seasonally dependent parameter sets enabled the model to capture seasonal behaviours of the hydrological process in a more realistic way. The use of seasonal parameters considered the influence of seasonality on a simplified model structure and physical processes such as infiltration, surface water flow, subsurface water flow, and baseflow. This made possible a better reproduction of soil moisture condition and runoff as initial conditions of a hydrological forecast or prediction. Therefore, season-based PDM-CEMADEN is better than the traditional model for the purpose of hydrological forecasting and prediction. An effective and efficient hydrological forecasting and prediction is highly important for optimal decision making by stakeholders. For example, the PDM-CEMADEN model was applied weekly for hydrological prediction of the Cantareira reservoir system from the water crisis in 2014 to the recovery of dead volume at the end of 2015 (Figure S9). Consequently, the added complexity of the season-based PDM-CEMADEN relative to the traditional model is well justified.

This study identified a distinct seasonal difference in calibration parameters of the season-based PDM-CEMADEN, although the difference varied among the study basins. During the wet season, the study basins have a larger capacity and variation of soil water storage, larger soil water conductivity, and quicker surface water flow than those during the dry season. The seasonality is evident in the larger values of the c_{max} and b parameters, and smaller values of the k_g and

k_2 parameters, for the wet season. Seasonal differences in climate, soil, land use, vegetation, and simplified model structure are the main conceptual/physical reasons for the routing parameters being seasonally dependent. The season-based PDM-CEMADEN parameters are comparable with the previous PDM hydrological simulations from Cabus (2008) and Samain and Pauwels (2013). However, compared with season-based PDM-CEMADEN, the traditional model obtained parameters with values compromised to the varying seasonality.

Further research should be dedicated to producing a better estimation of the AET for an improved season-based PDM-CEMADEN simulation. Seasonal calibration should consider different relations between AET/PET and soil moisture deficit through the use of different values of b_e for different seasons. If available, the LAI should be included in the rainfall–runoff modelling to consider the effects of seasonal changes in land use and vegetation. The model is to be tested in other Brazilian basins under different conditions of climatology, land use, soil, geology, and size. Then, regionalization of the derived parameters makes possible its application to ungauged basins (McIntyre et al., 2005; Vleeschouwer & Pauwels, 2013). For the ungauged river flow forecasting problem, the PDM principles can be used in its grid-based formulation and strong spatial data support on terrain, land cover, soil, and geology properties to shape the flood response everywhere across a catchment or countrywide model domain (Cole & Moore, 2009; Moore, Cole, Bell, & Jones, 2006). Finally, data assimilation promotes its application for real-time runoff forecasting and medium-term runoff prediction of all Brazilian basins (Alvarez-Garreton, Ryu, Western, Crow, & Robertson, 2014), which facilitates stakeholder decision making for both water resource management and natural disaster prevention.

ORCID

Rong Zhang http://orcid.org/0000-0002-5816-3959

REFERENCES

Alvares, C. A., Stape, J. L., Sentelhas, P. C., de Moraes, G., Leonardo, J., & Gerd, S. (2013). Köppen's climate classification map for Brazil. *Meteorologische Zeitschrift*, *22*(6), 711–728. https://doi.org/10.1127/0941-2948/2013/0507

Alvarez-Garreton, C., Ryu, D., Western, A. W., Crow, W. T., & Robertson, D. E. (2014). The impacts of assimilating satellite soil moisture into a rainfall–runoff model in a semi-arid catchment. *Journal of Hydrology*, *519*, 2763–2774. https://doi.org/10.1016/j.jhydrol.2014.07.041

Arnoldus, H. M. J., Boodt, M. D., & Gabriels, D. (1980). An approximation of the rainfall factor in the Universal Soil Loss Equation. *Assessment of Erosion*, 127–132.

Bekele, E. G., & Nicklow, J. W. (2007). Multi-objective automatic calibration of SWAT using NSGA-II. *Journal of Hydrology*, *341*(3–4), 165–176. https://doi.org/10.1016/j.jhydrol.2007.05.014

Bennett, J. C., Robertson, D. E., Ward, P. G. D., Hapuarachchi, H. A. P., & Wang, Q. J. (2016). Calibrating hourly rainfall–runoff models with daily forcings for streamflow forecasting applications in meso-scale catchments. *Environmental Modelling & Software*, *76*, 20–36. https://doi.org/10.1016/j.envsoft.2015.11.006

Best, M. J., Pryor, M., Clark, D. B., Rooney, G. G., Essery, R. L. H., Ménard, C. B., … Harding, R. J. (2011). The Joint UK Land Environment Simulator (JULES), model description—Part 1: Energy and water fluxes. *Geoscientific Model Development*, *4*(3), 677–699. https://doi.org/10.5194/gmd-4-677-2011

Brown, A. E., Zhang, L., McMahon, T. A., Western, A. W., & Vertessy, R. A. (2005). A review of paired catchment studies for determining changes in water yield resulting from alterations in vegetation. *Journal of Hydrology*, *310*(1), 28–61. https://doi.org/10.1016/j.jhydrol.2004.12.010

Cabus, P. (2008). River flow prediction through rainfall–runoff modelling with a probability-distributed model (PDM) in Flanders, Belgium. *Agricultural Water Management*, *95*(7), 859–868. https://doi.org/10.1016/j.agwat.2008.02.013

Coelho, C. A., Cardoso, D. H. F., & Firpo, M. A. F. (2016). Precipitation diagnostics of an exceptionally dry event in São Paulo, Brazil. *Theoretical and Applied Climatology*, *125*(3–4), 769–784. https://doi.org/10.1007/s00704-015-1540-9

Cole, S. J., & Moore, R. J. (2009). Distributed hydrological modelling using weather radar in gauged and ungauged basins. *Advances in Water Resources*, *32*(7), 1107–1120. https://doi.org/10.1016/j.advwatres.2009.01.006

Cuartas, L. A. (2008). Estudo observacional e de modelagem hidrológica de uma micro-bacia em floresta não perturbada na Amazônia Central. Diss. *PhD thesis*, INPE, Sao Jose dos Campos, Brazil.

da Silva, A. M. (2004). Rainfall erosivity map for Brazil. *Catena*, *57*(3), 251–259. https://doi.org/10.1016/j.catena.2003.11.006

de Vos, N. J., Rientjes, T. H. M., & Gupta, H. V. (2010). Diagnostic evaluation of conceptual rainfall–runoff models using temporal clustering. *Hydrological Processes*, *24*(20), 2840–2850. https://doi.org/10.1002/hyp.7698

Deb, K., Pratap, A., Agarwal, S., & Meyarivan, T. A. M. T. (2002). A fast and elitist multiobjective genetic algorithm: NSGA-II. *IEEE Transactions on Evolutionary Computation*, *6*(2), 182–197. https://doi.org/10.1109/4235.996017

Dingman, S. L. (2015). *Physical hydrology*. Long Grove: Waveland Press.

Dooge, J. (1973). Linear theory of hydrologic systems (no. 1468). Agricultural Research Service, US Department of Agriculture.

Fan, F. M., Collischonn, W., Meller, A., & Botelho, L. C. M. (2014). Ensemble streamflow forecasting experiments in a tropical basin: The São Francisco river case study. *Journal of Hydrology*, *519*(D), 2906–2919. https://doi.org/10.1016/j.jhydrol.2014.04.038

Fatichi, S., Ivanov, V. Y., & Caporali, E. (2012). Investigating interannual variability of precipitation at the global scale: Is there a connection with seasonality? *Journal of Climate*, *25*(16), 5512–5523. https://doi.org/10.1175/JCLI-D-11-00356.1

Fournier, H. (1960). *Climat et érosion*. Paris: Presses Universitaires de France.

García-Marín, A. P., Ayuso-Mu oz, J. L., Cantero, F. N., & Ayuso-Ruiz, J. L. (2017). Spatial and trend analyses of rainfall seasonality and erosivity in the west of Andalusia (period 1945–2005). *Soil Science*, *182*(4), 146–158. https://doi.org/10.1097/SS.0000000000000206

Getirana, A. (2016). Extreme water deficit in Brazil detected from space. *Journal of Hydrometeorology*, *17*(2), 591–599. https://doi.org/10.1175/JHM-D-15-0096.1

Grimm, A. M. (2011). Interannual climate variability in South America: Impacts on seasonal precipitation, extreme events, and possible effects of climate change. *Stochastic Environmental Research and Risk Assessment*, 25(4), 537–554. https://doi.org/10.1007/s00477-010-0420-1-554

Hargreaves, G. H., & Allen, R. G. (2003). History and evaluation of Hargreaves evapotranspiration equation. *Journal of Irrigation and Drainage Engineering*, 129(1), 53–63. https://doi.org/10.1061/(ASCE)0733-9437

Kim, H. S., & Lee, S. (2014). Assessment of a seasonal calibration technique using multiple objectives in rainfall–runoff analysis. *Hydrological Processes*, 28(4), 2159–2173. https://doi.org/10.1002/hyp.9785-2173

Kim, K. B., & Han, D. (2017). Exploration of sub-annual calibration schemes of hydrological models. *Hydrology Research*, 48(4), 1014–1031. https://doi.org/10.2166/nh.2016.296

Kim, K. B., Kwon, H. H., & Han, D. (2016). Hydrological modelling under climate change considering nonstationarity and seasonal effects. *Hydrology Research*, 47(2), 260–273.

Krause, P., Boyle, D. P., & Bäse, F. (2005). Comparison of different efficiency criteria for hydrological model assessment. *Advances in Geosciences*, 5, 89–97. https://doi.org/10.5194/adgeo-5-89-2005

Liu, J., Wang, J., Pan, S., Tang, K., Li, C., & Han, D. (2015). A real-time flood forecasting system with dual updating of the NWP rainfall and the river flow. *Natural Hazards*, 77(2), 1161–1182. https://doi.org/10.1007/s11069-015-1643-8

Luo, J., Wang, E., Shen, S., Zheng, H., & Zhang, Y. (2012). Effects of conditional parameterization on performance of rainfall–runoff model regarding hydrologic non-stationarity. *Hydrological Processes*, 26(26), 3953–3961. https://doi.org/10.1002/hyp.8420

McIntyre, N., Lee, H., Wheater, H., Young, A., & Wagener, T. (2005). Ensemble predictions of runoff in ungauged catchments. *Water Resources Research*, 41(12). https://doi.org/10.1029/2005WR004289

Merz, R., Parajka, J., & Blöschl, G. (2011). Time stability of catchment model parameters: Implications for climate impact analyses. *Water Resources Research*, 47(2). https://doi.org/10.1029/2010WR009505

Moore, R. J. (1985). The probability-distributed principle and runoff production at point and basin scales. *Hydrological Sciences Journal*, 30(2), 273–297. https://doi.org/10.1080/02626668509490989

Moore, R. J. (1999). Real-time flood forecasting systems: Perspectives and prospects. In *Floods and landslides: Integrated risk assessment* (pp. 147–189). Berlin: Springer Berlin Heidelberg.

Moore, R. J. (2007). The PDM rainfall–runoff model. *Hydrology and Earth System Sciences*, 11(1), 483–499. https://doi.org/10.5194/hess-11-483-2007

Moore, R. J., & Bell, V. A. (2002). Incorporation of groundwater losses and well level data in rainfall–runoff models illustrated using the PDM. *Hydrology and Earth System Sciences*, 6(1), 25–38. https://doi.org/10.5194/hess-6-25-2002

Moore, R. J., Cole, S. J., Bell, V. A., & Jones, D. A. (2006). Issues in flood forecasting: Ungauged basins, extreme floods and uncertainty. In I. Tchiguirinskaia, K. N. N. Thein, & P. Hubert (Eds.), *Frontiers in flood research* (Vol. 305)8th Kovacs Colloquium, UNESCO (pp. 103–122). Paris, June/July 2006: IAHS Publ.

Moriasi, D. N., Arnold, J. G., Van Liew, M. W., Bingner, R. L., Harmel, R. D., & Veith, T. L. (2007). Model evaluation guidelines for systematic quantification of accuracy in watershed simulations. *Transactions of the ASABE*, 50(3), 885–900. https://doi.org/10.13031/2013.23153

Muleta, M. K. (2012). Improving model performance using season-based evaluation. *Journal of Hydrologic Engineering*, 17(1), 191–200. https://doi.org/10.1061/(ASCE)HE.1943-5584.0000421

Nash, J. E., & Sutcliffe, J. V. (1970). River flow forecasting through conceptual models part I—A discussion of principles. *Journal of Hydrology*, 10(3), 282–290. https://doi.org/10.1016/0022-1694(70)90255-6

Nobre, C. A., Marengo, J. A., Seluchi, M. E., Cuartas, L. A., & Alves, L. M. (2016). Some characteristics and impacts of the drought and water crisis in southeastern Brazil during 2014 and 2015. *Journal of Water Resource and Protection*, 8(02), 252–262. https://doi.org/10.4236/jwarp.2016.82022

O'Connor, K. M. (1982). Derivation of discretely coincident forms of continuous linear time-invariant models using the transfer function approach. *Journal of Hydrology*, 59(1–2), 1–48. https://doi.org/10.1016/0022-1694(82)90002-6

Oliver, J. E. (1980). Monthly precipitation distribution: A comparative index. *The Professional Geographer*, 32(3), 300–309. https://doi.org/10.1111/j.0033-0124.1980.00300.x

Paik, K., Kim, J. H., Kim, H. S., & Lee, D. R. (2005). A conceptual rainfall–runoff model considering seasonal variation. *Hydrological Processes*, 19(19), 3837–3850. https://doi.org/10.1002/hyp.5984

Peel, M. C., Finlayson, B. L., & McMahon, T. A. (2007). Updated world map of the Köppen–Geiger climate classification. *Hydrology and Earth System Sciences*, 11, 1633–1644. https://doi.org/10.5194/hess-11-1633-2007

Rao, V. B., Franchito, S. H., Santo, C. M. E., & Gan, M. A. (2016). An update on the rainfall characteristics of Brazil: Seasonal variations and trends in 1979–2011. *International Journal Climatology*, 36(1), 291–302. https://doi.org/10.1002/joc.4345

Samain, B., & Pauwels, V. R. N. (2013). Impact of potential and (scintillometer-based) actual evapotranspiration estimates on the performance of a lumped rainfall–runoff model. *Hydrology and Earth System Sciences*, 17(11), 4525–4540. https://doi.org/10.5194/hess-17-4525-2013

Seiller, G., Anctil, F., & Perrin, C. (2012). Multimodel evaluation of twenty lumped hydrological models under contrasted climate conditions. *Hydrology and Earth System Sciences*, 16(4), 1171–1189. https://doi.org/10.5194/hess-16-1171-2012

Smith, J. M. (1977). *Mathematical modelling and digital simulation for engineers and scientists*. New York, NY, USA: John Wiley & Sons, Inc.

Tomasella, J., Hodnett, M. G., & Rossato, L. (2000). Pedotransfer functions for the estimation of soil water retention in Brazilian soils. *Soil Science Society of America Journal*, 64(1), 327–338. https://doi.org/10.2136/sssaj2000.641327x

Vleeschouwer, N. D., & Pauwels, V. R. (2013). Assessment of the indirect calibration of a rainfall–runoff model for ungauged catchments in Flanders. *Hydrology and Earth System Sciences*, 17(5), 2001–2016. https://doi.org/10.5194/hess-17-2001-2013

Walsh, R. P. D., & Lawler, D. M. (1981). Rainfall seasonality: description, spatial patterns and change through time. *Weather*, 36(7), 201–208. https://doi.org/10.1002/j.1477-8696.1981.tb05400.x

Zhang, D., Chen, X., Yao, H., & Lin, B. (2015). Improved calibration scheme of SWAT by separating wet and dry seasons. *Ecological Modelling*, 301, 54–61. https://doi.org/10.1016/j.ecolmodel.2015.01.018

Zhang, R., Moreira, M., & Corte-Real, J. (2016). Multi-objective calibration of the physically based, spatially distributed SHETRAN hydrological model. *Journal of Hydroinformatics*, 18(3), 428–445. https://doi.org/10.2166/hydro.2015.219

SUPPORTING INFORMATION

Additional supporting information may be found online in the Supporting Information section at the end of the article.

How to cite this article: Zhang R, Cuartas LA, de Castro Carvalho LV, et al. Season-based rainfall–runoff modelling using the probability-distributed model (PDM) for large basins in southeastern Brazil. *Hydrological Processes*. 2018;32:2217–2230. https://doi.org/10.1002/hyp.13154